Geophys. J. Int. (2000) **140,** 51–62

Effects due to compressional and compositional density stratification on load-induced Maxwell viscoelastic perturbations

Detlef Wolf[1] and Georg Kaufmann[2]

[1] *GeoForschungsZentrum Potsdam, Division* 1: *Kinematics and Dynamics of the Earth, Telegrafenberg,* D-14473 *Potsdam, Germany*
[2] *Research School of Earth Sciences, Australian National University, Canberra* ACT 0200, *Australia*

Accepted 1999 July 27. Received 1999 April 30; in original form 1997 October 3

SUMMARY

Calculations of viscoelastic perturbations of an incompressible fluid earth initially in hydrostatic equilibrium have been conventionally based on models consisting of isocompositional layers. A special case is the incompressible, isocompositional half-space, for which the initial density distribution is *spatially uniform*. One of the deficiencies of this model is that it ignores the increase of the initial density with depth in the earth's interior due to *compressional* and *compositional* stratification.

The present study is concerned with load-induced Maxwell viscoelastic perturbations of a half-space with a compressional and compositional initial density gradient. *Analytic solutions* to this problem are deduced for the limiting cases of purely compressional stratification (earth model P) and purely compositional stratification (earth model C).

The comparison of the solutions for these earth models with that for the special case of no density stratification (earth model R) shows that effects due to the initial density gradient become important for perturbations whose lateral scale length exceeds about 10^3 km. Using axisymmetric models of the Pleistocene *Fennoscandian* and *Canadian ice sheets* and considering the vertical surface displacements near the load axes, the maximum differences are found to be about 10 m (Fennoscandia) or 35 m (Canada) at the beginning of relaxation for earth models P and R and about 50 m (Fennoscandia) or 150 m (Canada) at intermediate times of relaxation for earth models C and R.

Key words: Canadian ice sheet, density, Fennoscandian ice sheet, glacial rebound, isostasy, viscoelasticity.

1 INTRODUCTION

For geodynamic processes of intermediate periods (e.g. glacial–isostatic adjustment, long-period tidal deformation), it is necessary to account for the deviations from elasticity in the earth's interior. As long as the anelastic response can be described by a *linear–viscoelastic* constitutive equation, the formulation of the incremental field theory of viscoelastodynamics is straightforward and solutions can be derived by means of Laplace-transform methods (Peltier 1974; Wu & Peltier 1982). The initial state has usually been assumed to be hydrostatic and can be included in the theory in two ways. One way is to parametrize seismologically inferred spherically symmetric earth models in terms of density, pressure and gravity, which is the approach taken by Peltier and most of his followers. The other way is to determine the initial state by solving suitable state equations. This approach is less common but allows the explicit discrimination between different types of stratification, e.g. *compressional* stratification due to self-compression of the material and *compositional* stratification due to chemical heterogeneity of the material.

Solutions for perturbations of a spherical earth model with a compressional initial density gradient specified by a state equation were given by Li & Yuen (1987) and Wu & Yuen (1991). Since their analyses were restricted to *viscous* perturbations of the initial state, the problem was simplified and solutions could be readily obtained without recourse to Laplace-transform methods. Later, Wolf (1991a, 1997) generalized the theory of viscoelastodynamics in order to allow for an arbitrary initial state. In particular, he showed that Laplace transform methods can be extended to include a compressible initial state. However, no explicit solutions of the field equations were given for this case.

A different type of compressibility was considered by Wolf (1985a) for a viscoelastic half-space and later by Vermeersen *et al.* (1996a), Vermeersen & Sabadini (1998), Hanyk *et al.* (1999) and Wieczerkowski (1999) for a self-gravitating viscoelastic sphere. In contrast to Li & Yuen (1987) and Wu & Yuen (1991), these investigators took the initial density as spatially homogeneous, but accounted for compressibility when modelling the viscoelastic perturbations. Although this does not constitute a physically self-consistent treatment of compressibility,

their studies serve to illuminate the problem of compressibility in general and to isolate the effects due to compressible perturbations in particular.

An intriguing topic is that of the appropriate mathematical treatment of earth models with continuous variations of the viscoelastic parameters with depth. This problem was originally considered in the geophysical literature by Parsons (1972, pp. 67–87) for a viscous half-space and has recently received renewed attention for self-gravitating viscoelastic spheres (e.g. Fang & Hager 1994, 1995; Han & Wahr 1995; Hanyk *et al.* 1995; Vermeersen *et al.* 1996b). A central question of the recent discussion has been whether earth models consisting of homogeneous layers are adequate representations of continuously stratified models.

The present study is concerned with viscoelastic earth models with continuous density stratification. In particular, the density increase with depth is assumed to be the *total* of compressional and compositional stratification. The purpose is to show that it is important to specify the type of density stratification in the initial state in order that physically meaningful equations governing the incremental state are obtained. In agreement with the modest objectives of the present study, the earth model is therefore kept simple. Hence, we use the model of a plane half-space perturbed by an axisymmetric surface load. Since effects due to the associated perturbation of the gravity field are small for deformations amenable to the half-space approximation (Cathles 1975, pp. 72–83; Amelung & Wolf 1994), the gravity field is taken as prescribed.

Following this introduction, the initial and incremental field equations and interface conditions appropriate to an initial density gradient produced by a combination of compressional and compositional stratification are collected (Section 2). After that, the analytic solutions to the equations are deduced (Section 3). The solution functions are studied more closely for the special cases of no density stratification (earth model R), compressional density stratification (earth model P) and compositional density stratification (earth model C) (Section 4). Finally, the main results of the study are summarized (Section 5).

2 FIELD EQUATIONS AND INTERFACE CONDITIONS

2.1 Tensor equations

2.1.1 Kinematics and notational conventions

We consider Cartesian tensor fields in indicial notation and use the summation convention: *index* subscripts i, j, k run over 1, 2, 3 and index subscripts repeated in any term imply summation over this range. We also employ the differentiation convention: index subscripts preceded by a comma denote partial differentiation with respect to the coordinate direction indicated by the subscript.

Using these conventions, we further consider an arbitrary field quantity describing some aspect of the state of a fluid. In particular, we use the *Lagrangian* formulation, $f_{ij\ldots}(\mathbf{X}, t)$, of this field quantity, which specifies the value of the field at the current particle position, $r_i(\mathbf{X}, t)$, as a function of the initial particle position, $X_i := r_i(\mathbf{X}, 0)$, and the current time, t. In the following, we assume that $X_i \in \mathscr{X}^3$, where $\mathscr{X}^3$ is the 3-D Euclidian domain and $t \in [0, \infty)$. We further assume that $\mathscr{X}^3$ can be decomposed into two open 3-D subdomains, $\mathscr{X}^3_-$ and $\mathscr{X}^3_+$, and the 2-D interface, $\mathscr{X}^2$, such that $\mathscr{X}^3 = \mathscr{X}^3_- \cup \mathscr{X}^3_+ \cup \mathscr{X}^2$ applies. In the present study, we assume that $f_{ij\ldots}(\mathbf{X}, t)$ is continuous for $X_i \in \mathscr{X}^3_- \cup \mathscr{X}^3_+$, but may be discontinuous for $X_i \in \mathscr{X}^2$.

For $X_i \in \mathscr{X}^3_- \cup \mathscr{X}^3_+$, the *current* field, $f_{ij\ldots}(\mathbf{X}, t)$, can be decomposed into *initial* and *incremental* fields according to $f_{ij\ldots}(\mathbf{X}, t) = f_{ij\ldots}(\mathbf{X}, 0) + f^{(\delta)}_{ij\ldots}(\mathbf{X}, t)$. In view of the definition of the Lagrangian formulation, the *material* incremental field, $f^{(\delta)}_{ij\ldots}(\mathbf{X}, t)$, describes the increment of $f_{ij\ldots}(\mathbf{X}, t)$ observed at the particle initially at X_i. Alternatively, the *local* incremental field, $f^{(\Delta)}_{ij\ldots}(\mathbf{X}, t)$, may be used, which describes the increment of $f_{ij\ldots}(\mathbf{X}, t)$ observed at X_i. Material and local increments are related by

$$f^{(\delta)}_{ij\ldots}(\mathbf{X}, t) = f^{(\Delta)}_{ij\ldots}(\mathbf{X}, t) + f_{ij\ldots,k}(\mathbf{X}, 0)\, u_k(\mathbf{X}, t) + \ldots , \tag{1}$$

where $u_i(\mathbf{X}, t) = r_i(\mathbf{X}, t) - r_i(\mathbf{X}, 0)$ is the displacement and $f_{ij\ldots,k}(\mathbf{X}, 0)\, u_k(\mathbf{X}, t)$ the *advective* incremental field.

The potentially discontinuous behaviour of $f_{ij\ldots}(\mathbf{X}, t)$ for $X_i \in \mathscr{X}^2$ is expressed by

$$[f_{ij\ldots}(\mathbf{X}, t)]^+_- := [f_{ij\ldots}(\mathbf{X}, t)]_+ - [f_{ij\ldots}(\mathbf{X}, t)]_- , \tag{2}$$

where $[f_{ij\ldots}(\mathbf{X}, t)]_+$ and $[f_{ij\ldots}(\mathbf{X}, t)]_-$ denote the limits of $f_{ij\ldots}(\mathbf{X}, t)$ for the positive and negative sides, respectively, of $\mathscr{X}^2$.

In the following, we consider a simplified mechanical field theory applying the assumption that the fluid is isentropic for $X_i \in \mathscr{X}^3_-$ and $X_i \in \mathscr{X}^3_+$, respectively, but may possess *compressional* and *compositional* stratification in these domains. We further suppose that the fluid is non-rotating, externally gravitating and subject only to gravitational volume forces. For the field equations and interface conditions stated below, $X_i \in \mathscr{X}^3_- \cup \mathscr{X}^3_+$ and $X_i \in \mathscr{X}^2$, respectively, are always implied. For notational convenience, the arguments X_i and t are suppressed and the argument $t = 0$ is displayed as the superscript (0) appended to the function symbol from now on.

2.1.2 Equations for the initial fields

Assuming that the fluid is initially in a state of hydrostatic equilibrium and considering the assumptions and conventions specified above, the initial field equations take the forms

$$-p^{(0)}_{,i} + g_i \rho^{(0)} = 0 , \tag{3}$$

$$\rho^{(0)} = \xi(p^{(0)}, c^{(0)}) , \tag{4}$$

where g_i denotes the gravity, p the (mechanical) pressure, c the (chemical) composition, ρ the volume mass density and ξ the state function. To decouple (3) and (4), consider the gradient of (4):

$$\rho^{(0)}_{,i} = \left(\frac{\partial \xi}{\partial p}\right)^{(0)} p^{(0)}_{,i} + \left(\frac{\partial \xi}{\partial c}\right)^{(0)} c^{(0)}_{,i} , \tag{5}$$

where $(\partial \xi / \partial p)^{(0)} := [\partial \xi / \partial p]_{p = p^{(0)}}$ and $(\partial \xi / \partial c)^{(0)} := [\partial \xi / \partial c]_{c = c^{(0)}}$. Also define

$$\frac{\rho^{(0)}}{\kappa} := \left(\frac{\partial \xi}{\partial p}\right)^{(0)} , \tag{6}$$

$$\lambda_i := \left(\frac{\partial \xi}{\partial c}\right)^{(0)} c^{(0)}_{,i} , \tag{7}$$

with κ the isentropic bulk modulus and λ_i the compositional initial density gradient. The ratio $\kappa/\rho^{(0)}$ is also referred to as the seismic parameter. Comparison of (3)–(7) yields

$$\rho^{(0)}_{,i} - \frac{\rho^{(0)}}{\kappa}\, g_i \rho^{(0)} - \lambda_i = 0\,. \tag{8}$$

This is a generalized form of the Williamson–Adams equation (Williamson & Adams 1923; Adams & Williamson 1924; Bullen 1975, pp. 67–68), which includes a compositional initial density gradient, λ_i. A comparison of (8) with a similar expression by Birch (1952, eq. 7) shows that λ_i corresponds to the non-isentropic initial density gradient, $\chi\rho^{(0)}\tau_i$, in his equation, with χ the thermal expansivity and τ_i the non-isentropic temperature gradient. Thus, non-isentropic stratification can be treated in complete analogy to compositional stratification (see also Wolf 1997, pp. 28-29). However, according to Birch (1952, 1964), the combined contribution of non-isentropic and compositional stratification does not amount to more than 10–20 per cent of that of the compressional stratification. In view of the limited objectives of the present study, we do not explicitly consider non-isentropic stratification. Then, with g_i, κ and λ_i prescribed, (3) and (8) are an overdetermined system of partial differential equations to be solved for $p^{(0)}$ and $\rho^{(0)}$. The initial interface conditions to be satisfied by the solution are

$$[p^{(0)}]^+_- = 0\,, \tag{9}$$

$$[\rho^{(0)}]^+_- = \text{finite}\,. \tag{10}$$

2.1.3 *Equations for the incremental fields:* (X_i, t) *domain*

Considering infinitesimal, isentropic, quasi-static linear–viscoelastic perturbations of a fluid and neglecting compositional changes and bulk relaxation, the local form of the momentum, constitutive, state and continuity equations, respectively, can be written as

$$t^{(\Delta)}_{ij,j} + g_i \rho^{(\Delta)} = 0\,, \tag{11}$$

$$t^{(\Delta)}_{ij} = \delta_{ij}(p^{(0)}_{,k} u_k + \kappa u_{k,k}) + \int_0^t \mu(t-t')\, d_{t'} \left[u_{i,j}(t') + u_{j,i}(t') - \frac{2}{3}\,\delta_{ij} u_{k,k}(t') \right] dt'\,, \tag{12}$$

$$\rho^{(\Delta)} = \frac{\rho^{(0)}}{\kappa}\, p^{(\Delta)} - \lambda_i u_i\,, \tag{13}$$

$$\rho^{(\Delta)} = -(\rho^{(0)} u_i)_{,i}\,, \tag{14}$$

where t_{ij} is the Cauchy stress, μ is the shear-relaxation function and d_t the material time-derivative operator. Equating (13) and (14), we obtain

$$p^{(\Delta)} = -\frac{\kappa}{\rho^{(0)}} \left[(\rho^{(0)} u_i)_{,i} - \lambda_i u_i \right]. \tag{15}$$

Suppose now that (15) can be replaced by the simultaneous conditions

$$\kappa \to \infty\,, \tag{16}$$

$$(\rho^{(0)} u_i)_{,i} - \lambda_i u_i \to 0\,, \tag{17}$$

$$p^{(\Delta)} = \text{finite}\,. \tag{18}$$

The significance of (17) becomes evident noting that, by (14), it can be recast into $\rho^{(\Delta)} \to -\lambda_i u_i$, which, by (1), is equivalent to $\rho^{(\delta)} \to (\rho^{(0)}_{,i} - \lambda_i) u_i$. Eq. (17) thus states that the dilatation of a displaced particle is constrained to the extent that the local incremental density equals the negative of the compositional initial density gradient or, equivalently, that the material incremental density exactly follows the compressional initial density gradient. We refer to this approximation as *local incremental incompressibility*. The same approximation has also been employed for studying long-period viscous perturbations of the Earth's mantle (e.g. Li & Yuen 1987; Wu & Yuen 1991; Thoraval *et al.* 1994; Panasyuk *et al.* 1996). The adaptation of this approximation to viscoelastic perturbations in the present investigation must yield results of similar accuracy as the above studies in the long-period viscous regime of the response. In the short-period elastic regime of the response, the approximation is expected to be less accurate. However, in the elastic regime, it is in conformity with the assumption of quasi-static perturbations, which excludes the consideration of periods close to those of elastic free oscillations. Using the approximation of local incremental incompressibility, the local form of the incremental field equations and interface conditions reduces to

$$t^{(\Delta)}_{ij,j} - g_i \lambda_j u_j = 0\,, \tag{19}$$

$$t^{(\Delta)}_{ij} = -\delta_{ij} p^{(\Delta)} + \int_0^t \mu(t-t')\, d'_t \times \left[u_{i,j}(t') + u_{j,i}(t') - \frac{2}{3}\,\delta_{ij} u_{k,k}(t') \right] dt'\,, \tag{20}$$

$$u_{i,i} + \frac{\rho^{(0)}}{\kappa}\, g_i u_i = 0\,, \tag{21}$$

$$[u_i]^+_- = 0\,, \tag{22}$$

$$[n^{(0)}_j (t^{(\Delta)}_{ij} - \delta_{ij}\rho^{(0)} g_k u_k)]^+_- = -g_i \sigma\,, \tag{23}$$

where g_i is normal to $\mathscr{X}^2$ and directed to its positive side, n_i is the unit normal in the direction of g_i and σ is the incremental interface mass density. The incremental equations are to be solved for $p^{(\Delta)}$, $t^{(\Delta)}_{ij}$ and u_i. We observe that κ remains finite in (21). This is because κ has entered by substituting the Williamson–Adams equation, (8), into the local incremental incompressibility condition, (17). If the initial state is also taken as incompressible, then $\kappa \to \infty$ applies also in (21) and it reduces to the conventional incremental incompressibility condition, $u_{i,i} = 0$.

2.1.4 *Equations for the incremental fields:* (X_i, s) *domain*

As a first step towards a solution to (19)–(23), we take the Laplace transforms of the equations. The Laplace transform of an arbitrary function, $f(t)$, is defined by

$$\tilde{f}(s) := \int_0^\infty f(t)\, \mathrm{e}^{-st}\, dt\,, \tag{24}$$

where s is the Laplace frequency. Using some elementary consequences of (24) and taking $u_i \to 0$ for $t \to 0+$, we obtain from (19)–(23) the Laplace-transformed incremental field

equations and interface conditions:

$$\tilde{t}^{(\Delta)}_{ij,j} - g_i \lambda_j \tilde{u}_j = 0\,, \tag{25}$$

$$\tilde{t}^{(\Delta)}_{ij} = -\delta_{ij}\tilde{p}^{(\Delta)} + s\tilde{\mu}\left(\tilde{u}_{i,j} + \tilde{u}_{j,i} - \frac{2}{3}\,\delta_{ij}\tilde{u}_{k,k}\right), \tag{26}$$

$$\tilde{u}_{i,i} + \frac{\rho^{(0)}}{\kappa}\, g_i \tilde{u}_i = 0\,, \tag{27}$$

$$[\tilde{u}_i]^+_- = 0\,, \tag{28}$$

$$[n^{(0)}_j(\tilde{t}^{(\Delta)}_{ij} - \delta_{ij}\rho^{(0)} g_k \tilde{u}_k)]^+_- = -g_i\tilde{\sigma}\,. \tag{29}$$

As in the above equations, the argument of Laplace-transformed quantities will usually be suppressed. We may use (26) to eliminate $\tilde{t}^{(\Delta)}_{ij}$ from (25) and (29). With (27) we arrive at the following incremental field equations and interface conditions:

$$-\tilde{p}^{(\Delta)}_{,i} - \frac{1}{3}\, s\tilde{\mu}\left(\frac{\rho^{(0)}}{\kappa}\, g_j\tilde{u}_j\right)_{,i} + s\tilde{\mu}\tilde{u}_{i,jj} - g_i\lambda_j\tilde{u}_j + s\tilde{\mu}_{,j}\left(\tilde{u}_{i,j} + \tilde{u}_{j,i} + \frac{2\rho^{(0)}}{3\kappa}\,\delta_{ij} g_k \tilde{u}_k\right) = 0\,, \tag{30}$$

$$\tilde{u}_{i,i} + \frac{\rho^{(0)}}{\kappa}\, g_i\tilde{u}_i = 0\,, \tag{31}$$

$$[\tilde{u}_i]^+_- = 0\,, \tag{32}$$

$$\left[n^{(0)}_i\tilde{p}^{(\Delta)} + \frac{2}{3}\, s\tilde{\mu} n^{(0)}_i \tilde{u}_{j,j} - s\tilde{\mu} n^{(0)}_j(\tilde{u}_{i,j} + \tilde{u}_{j,i}) + n^{(0)}_i \rho^{(0)} g_j \tilde{u}_j\right]^+_- = g_i\tilde{\sigma}\,. \tag{33}$$

2.2 Scalar equations

2.2.1 *Symmetries and simplifications*

We now assume that the fluid is initially confined to $\mathscr{X}^3_+$, so that $p=0$, $\mu(t-t')=0$ and $\rho=0$ for $X_i \in \mathscr{X}^3_-$. It then follows from the incremental equations that u_i = continuous for $X_i \in \mathscr{X}^2$ and u_i = indeterminate for $X_i \in \mathscr{X}^3_-$ and that the remaining incremental quantities vanish identically for $X_i \in \mathscr{X}^3_-$. Furthermore, we consider the case that $\mathscr{X}^2$ is the horizontal plane. In applications to the Earth, this approximation is appropriate only to perturbations whose typical lateral wavelength is short compared to the Earth's radius. We choose cylindrical coordinates, $X_i = (r, \phi, z)$, and stipulate $\mathscr{X}^3_+ = \{X_i \,|\, z \in (0, \infty)\}$, whence $\mathscr{X}^2 = \{X_i \,|\, z = 0\}$. The fluid initially occupying $\mathscr{X}^3_+$ is referred to as a *half-space*, the material sheet initially coinciding with $\mathscr{X}^2$ as a *load* and the coordinate triple (r, ϕ, z) as an *observation point*; the coordinates r, ϕ and z are called *radial distance*, *azimuth* and *depth*, respectively. For convenience, we henceforth use

$$\gamma_i := \frac{\rho^{(0)}}{\kappa}\, g_i\,, \tag{34}$$

with γ_i the inverse compressional scale length. Since, in view of the assumption of initial hydrostatic equilibrium, g_i and λ_i are normal to $\mathscr{X}^2$, we may put in cylindrical coordinates $g_i = (0, 0, g)$, $n^{(0)}_i = (0, 0, 1)$, $\gamma_i = (0, 0, \gamma)$ and $\lambda_i = (0, 0, \lambda)$. To proceed more conveniently, we further simplify the problem and in the following assume that g, γ, λ and $\tilde{\mu}$ are spatially constant.

2.2.2 *Equations for the initial fields*

With the symmetries and simplifications introduced above, the relevant scalar components of (3) and (8)–(10) take the forms

$$-p^{(0)}_{,z} + g\rho^{(0)} = 0\,, \tag{35}$$

$$\rho^{(0)}_{,z} - \gamma\rho^{(0)} - \lambda = 0\,, \tag{36}$$

$$[p^{(0)}]_+ = 0\,, \tag{37}$$

$$[\rho^{(0)}]_+ = \rho^*\,, \tag{38}$$

with ρ^* the surface value of the initial density.

2.2.3 *Equations for the incremental fields:* (r, z, s) *domain*

In the following, we consider an axisymmetric load with the z-axis coinciding with the symmetry axis. From symmetry considerations, it then follows that $f_{,\phi} = 0$ and $u_\phi = 0$. Using $u := u_r$ for the radial displacement, $w := u_z$ for the downward displacement and the other symmetries and simplifications introduced above, the relevant scalar components of (30)–(33) take the forms

$$\tilde{p}^{(\Delta)}_{,r} - s\tilde{\mu}\left(\tilde{u}_{,rr} + \frac{1}{r}\,\tilde{u}_{,r} - \frac{1}{r^2}\,\tilde{u} + \tilde{u}_{,zz} - \frac{1}{3}\,\gamma\tilde{w}_{,r}\right) = 0\,, \tag{39}$$

$$\tilde{p}^{(\Delta)}_{,z} - s\tilde{\mu}\left(\tilde{w}_{,rr} + \frac{1}{r}\,\tilde{w}_{,r} + \tilde{w}_{,zz} - \frac{1}{3}\,\gamma\tilde{w}_{,z}\right) + g\lambda\tilde{w} = 0\,, \tag{40}$$

$$\tilde{u}_{,r} + \frac{1}{r}\,\tilde{u} + \tilde{w}_{,z} + \gamma\tilde{w} = 0\,, \tag{41}$$

$$[\tilde{u}_{,z} + \tilde{w}_{,r}]_+ = 0\,, \tag{42}$$

$$\left[\tilde{p}^{(\Delta)} - s\tilde{\mu}\left(\frac{2}{3}\,\gamma\tilde{w} + 2\tilde{w}_{,z}\right) + \rho^* g\tilde{w}\right]_+ = g\tilde{\sigma}\,. \tag{43}$$

Eqs (39)–(41) are three coupled second-order partial differential equations for $\tilde{p}^{(\Delta)}$, $\tilde{u}$ and $\tilde{w}$, which must be solved subject to (42) and (43). These equations are to be completed by conditions requiring that the incremental fields and their spatial derivatives remain bounded as $z \to \infty$.

In order to solve the equations, we introduce the rotation $\omega = (u_{,z} - w_{,r})/2$. This allows us to reduce (39)–(41) to the following first-order system:

$$\tilde{p}^{(\Delta)}_{,r} - 2s\tilde{\mu}\left(\tilde{\omega}_{,z} - \frac{2}{3}\,\gamma\tilde{w}_{,r}\right) = 0\,, \tag{44}$$

$$\tilde{p}^{(\Delta)}_{,z} + 2s\tilde{\mu}\left(\tilde{\omega}_{,r} + \frac{1}{r}\,\tilde{\omega} - \frac{2}{3}\,\gamma\tilde{u}_{,r} - \frac{2}{3r}\,\gamma\tilde{u} - \frac{2}{3}\,\gamma^2\tilde{w}\right) + g\lambda\tilde{w} = 0\,, \tag{45}$$

$$\tilde{u}_{,r} + \frac{1}{r}\,\tilde{u} + \tilde{w}_{,z} + \gamma\tilde{w} = 0\,, \tag{46}$$

$$\tilde{u}_{,z} - \tilde{w}_{,r} - 2\tilde{\omega} = 0\,. \tag{47}$$

2.2.4 *Equations for the incremental fields:* (k, z, s) *domain*

The equations can be decoupled by taking their Hankel transforms. The lth-order Hankel transform of an arbitrary function, $f(r)$, is defined by

$$F^{[l]}(k) := \int_0^\infty f(r) J_l(kr)\, r\, dr\,, \tag{48}$$

where k is the Hankel wavenumber. Using some elementary theorems for Hankel transforms (e.g. Sneddon 1951, pp. 60–62), (44)–(47) become

$$\partial_z \begin{bmatrix} \widetilde{U}^{[1]} \\ \widetilde{W}^{[0]} \\ \widetilde{\Omega}^{[1]} \\ \widetilde{P}^{(\Delta)[0]} \end{bmatrix} = \begin{bmatrix} 0 & -k & 2 & 0 \\ -k & -\gamma & 0 & 0 \\ 0 & -\frac{2}{3}\gamma k & 0 & -\frac{k}{2s\tilde{\mu}} \\ \frac{4}{3}\gamma s\tilde{\mu}k & \frac{4}{3}\gamma^2 s\tilde{\mu} - g\lambda & -2s\tilde{\mu}k & 0 \end{bmatrix} \times \begin{bmatrix} \widetilde{U}^{[1]} \\ \widetilde{W}^{[0]} \\ \widetilde{\Omega}^{[1]} \\ \widetilde{P}^{(\Delta)[0]} \end{bmatrix}. \tag{49}$$

The interface conditions take the forms

$$[\widetilde{U}^{[1]}_{,z} - k\widetilde{W}^{[0]}]_+ = 0, \tag{50}$$

$$\left[\widetilde{P}^{(\Delta)[0]} - s\tilde{\mu}\left(\frac{2}{3}\gamma\widetilde{W}^{[0]} + 2\widetilde{W}^{[0]}_{,z}\right) + \rho^* g\widetilde{W}^{[0]}\right]_+ = g\widetilde{\Sigma}^{[0]}. \tag{51}$$

In the following, the superscripts of the symbols are suppressed.

3 SOLUTIONS TO THE EQUATIONS

3.1 Initial fields

The solution to (35)–(38) subject to g, γ and λ being constant is

$$\rho^{(0)} = \left(\rho^* + \frac{\lambda}{\gamma}\right)\mathrm{e}^{\gamma z} - \frac{\lambda}{\gamma}, \tag{52}$$

$$p^{(0)} = \left(\frac{\rho^* g}{\gamma} + \frac{\lambda g}{\gamma^2}\right)(\mathrm{e}^{\gamma z} - 1) - \frac{\lambda g}{\gamma} z. \tag{53}$$

Since $\gamma z \ll 1$ for all depths of geophysical interest, we may write, correct to first order, $\mathrm{e}^{\gamma z} \simeq 1 + \gamma z$, such that (52) reduces to

$$\rho^{(0)} = \rho^* + (\gamma\rho^* + \lambda)z. \tag{54}$$

We briefly consider three special cases of (54) and compare them with the density stratification according to the PREM reference earth model (Dziewonski & Anderson 1981). If $\gamma = \lambda = 0$ (earth model R), we have an incompressible and isocompositional initial state and the initial density is spatially homogeneous, $\rho^{(0)} = \rho^*$. If $\gamma \neq 0$ and $\lambda = 0$ (earth model P), the initial density varies linearly as a result of the compressibility of the material. For standard parameter values (Table 1), the compressional density gradient is $\gamma\rho^* = 5.6 \times 10^{-4}$ kg m^{-4}. As a consequence, the initial density increases from its surface value of $\rho^* = 3380$ kg m^{-3} to a value of ~ 5000 kg m^{-3} at a depth of 2900 km. This is somewhat lower than the PREM density of 5545 kg m^{-3} above the core–mantle boundary. If $\gamma = 0$ and $\lambda \neq 0$ (earth model C), the linear variation of the initial density is due to compositional stratification alone. For a compressional gradient of $\lambda = 8 \times 10^{-4}$ kg m^{-4} (Table 1), the initial density reaches a value of ~ 5700 kg m^{-3} at a depth of 2900 km. The more realistic assumption of both compressional and compositional density gradients not considered here would require a strong reduction of the compositional gradient (Birch 1964).

Table 1. Standard parameter values used for earth models.

Quantity	Symbol	Value
Surface value of density	ρ^*	3380 kg m^{-3}
Compositional density gradient	λ	8.00×10^{-4} kg m^{-4}
Surface value of bulk modulus	κ^*	2.00×10^{11} Pa
Elastic shear modulus	$\mu^{(e)}$	1.45×10^{11} Pa
Viscosity	η	1.00×10^{21} Pa s
Gravity	g	9.81 m s^{-2}

3.2 Incremental fields: (k, z, s) domain

We assume a general solution of the form

$$[\widetilde{U}, \widetilde{W}, \widetilde{\Omega}, \widetilde{P}]^{\mathrm{T}} = [A_1, A_2, A_3, A_4]^{\mathrm{T}} \mathrm{e}^{mz}. \tag{55}$$

Necessary and sufficient for this solution to be non-trivial is that the characteristic equation of (49) be satisfied:

$$(m^2 + \gamma m - k^2)(m^2 - k^2) + \frac{g\lambda k^2}{s\tilde{\mu}} = 0. \tag{56}$$

This is a fourth-order equation in m, which has a simple solution only if $\lambda = 0$ (earth model P), $\gamma = 0$ (earth model C) or $\lambda = \gamma = 0$ (earth model R). In the following, these cases are considered individually.

3.2.1 *Earth model P*

If $\lambda = 0$, the characteristic equation has the following simple roots:

$$m_{1,2} = \pm k, \qquad m_{3,4} = -\frac{\gamma}{2} \pm \sqrt{k^2 + \frac{\gamma^2}{4}}, \tag{57}$$

which are the eigenvalues of the solution. The associated eigenvectors can be found using standard procedures (e.g. Gantmacher 1959, pp. 95–129). Requiring the boundedness of the fields for $z \to \infty$, the vectors associated with m_1 and m_3 are without significance and the general solution for the basic fields $\widetilde{W}$, $\widetilde{U}$ and $\widetilde{P}$ takes the form

$$\begin{bmatrix} \widetilde{W} \\ \widetilde{U} \\ \widetilde{P} \end{bmatrix} = \begin{bmatrix} k \\ -(\gamma + m_2) \\ -\frac{1}{3}\gamma s\tilde{\mu}k \end{bmatrix} B_2 \mathrm{e}^{m_2 z} + \begin{bmatrix} k \\ -(\gamma + m_4) \\ -\frac{4}{3}\gamma s\tilde{\mu}k \end{bmatrix} B_4 \mathrm{e}^{m_4 z}. \tag{58}$$

The free constants, B_2 and B_4, follow from the interface conditions, (50) and (52). We find

$$B_2 = \frac{2}{\gamma\left[2s\tilde{\mu}\left(l - \frac{\gamma}{2} - \frac{2kl}{\gamma} + \frac{2k^2}{\gamma}\right) + \rho^* g\right]} g\widetilde{\Sigma}, \tag{59}$$

$$B_4 = \frac{2\left(1 - \frac{\gamma}{2k}\right)}{\gamma\left[2s\tilde{\mu}\left(l - \frac{\gamma}{2} - \frac{2kl}{\gamma} + \frac{2k^2}{\gamma}\right) + \rho^* g\right]} g\widetilde{\Sigma}, \tag{60}$$

where $l=\sqrt{k^2+\gamma^2/4}$ has been used. Substitution of (59) and (60) into (58) yields in particular

$$[\widetilde{W}]_+ = \frac{g\widetilde{\Sigma}}{2s\tilde{\mu}\epsilon k+\rho^* g}\,, \tag{61}$$

with the compressional coefficient, ϵ, given by

$$\epsilon = \frac{2k}{\gamma}-\frac{\gamma}{2k}+\sqrt{1+\frac{\gamma^2}{4k^2}}-\sqrt{1+\frac{4k^2}{\gamma^2}}\,. \tag{62}$$

In Fig. 1, $\epsilon(n)$ is shown for three surface values of the bulk modulus, κ^*, which, in view of $\gamma=\rho^{(0)}g/\kappa$, corresponds to three density stratifications. Here and in the following, we use the normalized Hankel wavenumber, $n:=ka$, with a the earth radius. The values of ϵ are confined to the interval $(-1, 1]$. They are non-decreasing for increasing n, with the zero-crossing shifting to smaller n if κ^* increases.

3.2.2 Earth model C

If $\gamma=0$, the characteristic equation has the following simple roots:

$$m_{1,2} = \pm k\sqrt{1+i\sqrt{\frac{\lambda g}{s\tilde{\mu}k^2}}}\,, \tag{63}$$

$$m_{3,4} = \pm k\sqrt{1-i\sqrt{\frac{\lambda g}{s\tilde{\mu}k^2}}}\,. \tag{64}$$

The eigenvectors associated with the eigenvalues are calculated as above. In order that the fields remain bounded as $z\to\infty$, the vectors associated with m_1 and m_3 are not required and the general solution for the basic fields $\widetilde{W}$, $\widetilde{U}$ and $\widetilde{P}$ reduces to

$$\begin{bmatrix}\widetilde{W}\\ \widetilde{U}\\ \widetilde{P}\end{bmatrix} = \begin{bmatrix}k^2\\ -m_2k\\ s\tilde{\mu}m_2(m_2^2-k^2)\end{bmatrix} B_2\,\mathrm{e}^{m_2z}+\begin{bmatrix}k^2\\ -m_4k\\ s\tilde{\mu}m_4(m_4^2-k^2)\end{bmatrix} B_4\,\mathrm{e}^{m_4z}\,. \tag{65}$$

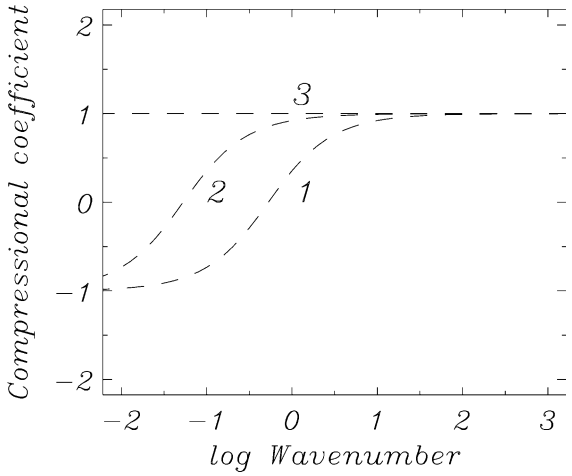

Figure 1. Compressional coefficient, ϵ, as a function of the normalized Hankel wavenumber, n. Results apply to $\kappa^*=1\times10^{11}$ Pa (curve 1), $\kappa^*=1\times10^{12}$ Pa (curve 2) and $\kappa^*\to\infty$ (curve 3); the other parameter values are given in Table 1.

Using the interface conditions, (50) and (52), the free constants, B_2 and B_4, become

$$B_2 = \frac{m_4^2+k^2}{s\tilde{\mu}[m_4(m_2^2+k^2)^2-m_2(m_4^2+k^2)^2]+\rho^* gk^2(m_4^2-m_2^2)}\,g\widetilde{\Sigma}\,, \tag{66}$$

$$B_4 = \frac{m_2^2+k^2}{s\tilde{\mu}[m_2(m_4^2+k^2)^2-m_4(m_2^2+k^2)^2]+\rho^* gk^2(m_2^2-m_4^2)}\,g\widetilde{\Sigma}\,. \tag{67}$$

Substitution of (66) and (67) into (65) gives in particular

$$[\widetilde{W}]_+ = \frac{g\widetilde{\Sigma}}{2s\tilde{\mu}\delta k+\rho^* g}\,, \tag{68}$$

where the k- and s-dependent compositional coefficient, δ, is given by

$$\delta = 2\sqrt[4]{1+\zeta^2}\left[\cos\frac{\vartheta}{2}+\frac{1}{2}\left(\frac{\zeta}{2}-\frac{2}{\zeta}\right)\sin\frac{\vartheta}{2}\right], \tag{69}$$

$$\zeta = \sqrt{\frac{\lambda g}{s\tilde{\mu}k^2}}\,, \tag{70}$$

$$\vartheta = \tan^{-1}\zeta\,. \tag{71}$$

In Fig. 2, δ is shown as a function of $n:=ka$ for two values of s and three values of λ. The values of δ are confined to the interval $[1, \infty)$ and are non-increasing for increasing n or decreasing s.

3.2.3 Earth model R

If $\lambda=\gamma=0$, the characteristic equation has two double roots:

$$m_{1,2} = \pm k\,. \tag{72}$$

This degenerate eigenvalue problem has been considered before (Wolf 1985b,c, 1991b). Here, we only list the solution for the downward surface displacement,

$$[\widetilde{W}]_+ = \frac{g\widetilde{\Sigma}}{2s\tilde{\mu}k+\rho^* g}\,. \tag{73}$$

We note that this also follows from (61) and (62) for $\gamma\to0$ or $\epsilon\to0$ and from (68)–(71) for $\lambda\to0$ or $\delta\to0$. In the following, we focus on the solutions for earth models P and C and recover the behaviour for earth model R by taking the appropriate limits.

4 VERTICAL SURFACE DISPLACEMENT

4.1 Maxwell viscoelasticity and Heaviside loading

To proceed beyond (61), (68) and (73), we must specify $\tilde{\mu}$ and $\widetilde{\Sigma}$. As a simple example, we consider the shear-relaxation function for *Maxwellian* viscoelasticity (e.g. Wolf 1994, 1997):

$$\mu = \mu^{(\mathrm{e})}H(t)\,\mathrm{e}^{-\alpha t}\,, \tag{74}$$

with $\alpha=\mu^{(\mathrm{e})}/\eta$ the inverse Maxwell time, $\mu^{(\mathrm{e})}$ the shear modulus, η the viscosity and H the Heaviside step function. In

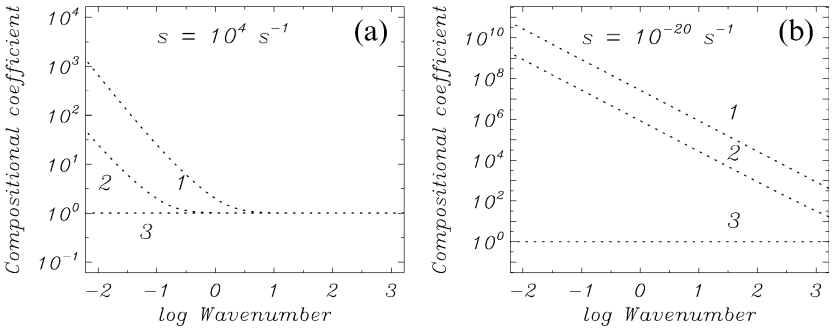

Figure 2. Compositional coefficient, δ, as a function of the normalized Hankel wavenumber, n, for (a) $s=1\times10^{4}$ s^{-1} and (b) $s=1\times10^{-20}$ s^{-1}. Results apply to $\lambda=8\times10^{-4}$ kg m^{-4} (curves 1), $\lambda=8\times10^{-6}$ kg m^{-4} (curves 2) and $\lambda\rightarrow0$ (curves 3); the other parameter values are given in Table 1.

the following, we consider *instantaneous* loading:

$$\Sigma=\Sigma' H(t)\,. \tag{75}$$

The Laplace transforms of (74) and (75) are

$$\tilde{\mu}=\frac{\mu^{(e)}}{s+\alpha}\,, \tag{76}$$

$$\tilde{\Sigma}=\frac{\Sigma'}{s}\,. \tag{77}$$

4.2 Transfer functions: (k, z, t) domain

We first introduce the viscoelastic transfer function in the (k, z, s) domain:

$$\tilde{T}^{(ve)}:=[\tilde{W}]_{+}\,\frac{\rho^{*}}{\Sigma'}\,. \tag{78}$$

Using this definition, we proceed by deriving explicit expressions of $\tilde{T}^{(ve)}$ for earth models P and C and by inverting these into the (k, z, t) domain.

4.2.1 *Earth model P*

In view of (61) and (76)–(78), we obtain

$$\tilde{T}^{(ve)}=\frac{1}{s}\,\frac{\rho^{*}g(s+\alpha)}{(2\mu^{(e)}\epsilon k+\rho^{*}g)s+\rho^{*}g\alpha}\,. \tag{79}$$

This can be recast into

$$\tilde{T}^{(ve)}=T^{(e)}\,\frac{1}{s}+T^{(v)}\left(\frac{1}{s}-\frac{1}{s+\beta}\right), \tag{80}$$

with

$$T^{(e)}=\frac{\rho^{*}g}{2\mu^{(e)}\epsilon k+\rho^{*}g}\,, \tag{81}$$

$$T^{(v)}=\frac{2\mu^{(e)}\epsilon k}{2\mu^{(e)}\epsilon k+\rho^{*}g}\,, \tag{82}$$

$$\beta=\frac{\rho^{*}g}{2\mu^{(e)}\epsilon k+\rho^{*}g}\,\alpha \tag{83}$$

the elastic amplitude, the viscous amplitude and the inverse relaxation time. The viscoelastic transfer function in the (k, z, t) domain, $T^{(ve)}$, follows upon taking the inverse Laplace transform of (80). This requires evaluation of the inverse Laplace integral (e.g. LePage 1980, pp. 318–322),

$$F(t)=\frac{1}{2\pi i}\int_{L}\tilde{F}(s)\,e^{st}\,ds\,, \tag{84}$$

for $\tilde{F}(s)=\tilde{T}^{(ve)}(s)$, where L is the Bromwich path. We obtain

$$T^{(ve)}=H(t)[T^{(e)}+T^{(v)}(1-e^{-\beta t})]\,. \tag{85}$$

For $\epsilon=1$, this reduces to the solution for earth model R (e.g. Wolf 1991b, eq. 107).

4.2.2 *Earth model C*

In view of (68) and (76)–(78), we get

$$\tilde{T}^{(ve)}=\frac{1}{s}\,\frac{\rho g^{*}(s+\alpha)}{(2\mu^{(e)}\delta k+\rho^{*}g)s+\rho^{*}g\alpha}\,. \tag{86}$$

In contrast to earth model P, the inverse Laplace transform of $\tilde{T}^{(ve)}$ for earth model C is not readily evaluated analytically. This is because the s dependence of the function δ is transcendental, so that elementary methods fail. Here, the inverse Laplace transformation is implemented numerically by means of the collocation method (e.g. Peltier 1974; Mitrovica & Peltier 1992).

4.3 Computation results: (k, z, t) domain

4.3.1 *General characteristics*

Fig. 3 shows the viscoelastic transfer functions, $T^{(ve)}$, for earth models R, P and C. The model parameters are given in Table 1. With $\kappa^{*}=2\times10^{11}$ Pa and $\lambda=8\times10^{-4}$ kg m^{-4}, the density gradients of earth models P and C, respectively, are similar to those in the earth's upper mantle.

For earth model R (Fig. 3a), $T^{(ve)}$ decreases with increasing n. For small times, $T^{(ve)}$ approaches 0 for n larger than about 10 but nearly reaches the value of 1 appropriate to the final state of hydrostatic equilibrium for n smaller than about 10^{-1}.

For earth model P (Fig. 3b), the behaviour of $T^{(ve)}$ is similar to that for earth model R provided that n is larger than about 10; however, for smaller n, the values of $T^{(ve)}$ exceed the corresponding values for earth model R significantly. We note in particular that, for very small times, $T^{(ve)}$ may even

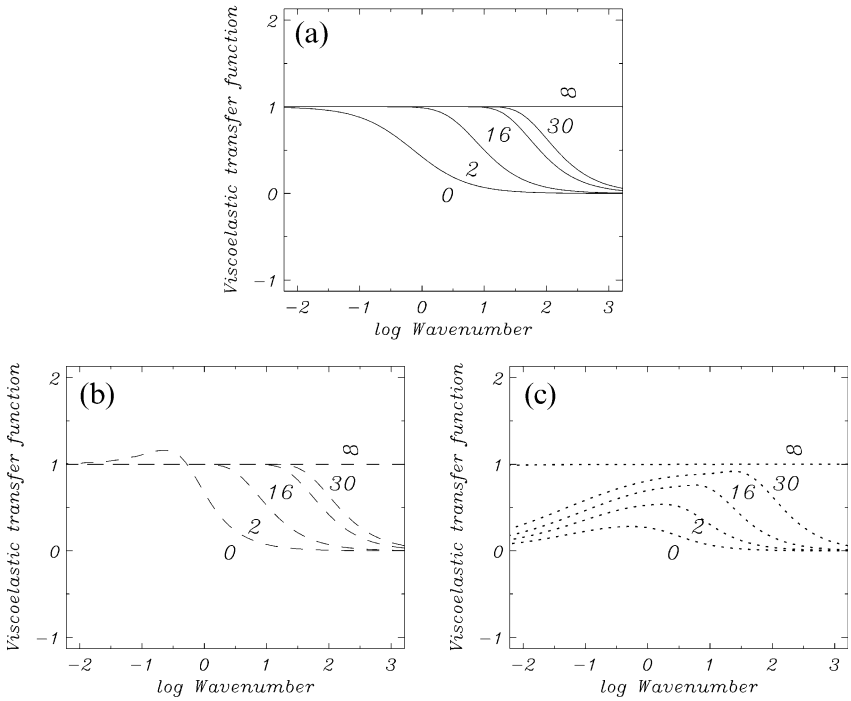

Figure 3. Viscoelastic transfer function, $T^{(ve)}$, as a function of the normalized Hankel wavenumber, n, for selected times (in units of ka) after onset of loading. Results apply to (a) earth model R, (b) earth model P and (c) earth model C. Parameter values are given Table 1.

exceed the value of 1 appropriate to the final state of hydrostatic equilibrium. This indicates that, for earth model P, the neglect of sphericity and self-gravitation becomes important for perturbations of very long wavelengths. However, the overshoot decays rapidly and has disappeared by about 2 ka. The closer distance between the curves for $t=0$ and $t=2$ ka for earth model P as compared to earth model R indicates the reduced relaxation time for the former model. For longer times, the differences between earth models R and P become very small.

The behaviour of earth model C is distinctly different. Thus, $T^{(ve)}$ remains small for small n. In addition, whereas the relaxation is similar to that for earth model R for n larger than about 10^2, it is strongly delayed for small n. For such wavenumbers, the final state of hydrostatic equilibrium is only reached after times exceeding the Maxwell time by several orders of magnitude.

In the following, the viscoelastic response of earth models P and C is discussed in greater detail.

4.3.2 Earth model P

Fig. 4 shows effects due to variations of $\mu^{(e)}$; the other parameters have their standard values (Table 1). Fig. 4 (top) applies to $\mu^{(e)}=1.45\times10^{11}$ Pa. Then, $\kappa^*/\mu^{(e)}\simeq1$, and we expect that compressibility contributes significantly to the response of earth model P. Compared to earth model R, the compressional density gradient enhances $T^{(e)}$ for n smaller than about 10. In the range $10^{-2}<n<1$, $T^{(e)}$ barely exceeds the value of 1, which is compensated by corresponding negative values of $T^{(v)}$. The behaviour of β^{-1} shows that the inclusion of a compressional density gradient slightly reduces the relaxation time for $n<10$. In Fig. 4 (bottom), $\mu^{(e)}$ is reduced to 1.45×10^{10} Pa. Since $\kappa^*/\mu^{(e)}\simeq10$, earth model P is effectively incompressible. As a result of this, its response is mainly determined by $\mu^{(e)}$ and the differences in $T^{(e)}$, $T^{(v)}$ and β^{-1} between earth models R and P are small. The reduction of $\mu^{(e)}$ by one order of magnitude tends to increase $T^{(e)}$ and β^{-1} for small n. However, for earth model P, the enhancement of $T^{(e)}$ is counteracted by a reduction resulting from the model's effectively incompressible response. Note in particular that the overshoot has almost disappeared.

Fig. 5 shows the influence of κ^* on the response; the other parameters continue to have their standard values (Table 1). In Fig. 5 (top), κ^* is increased to 2×10^{12} Pa. Then, $\kappa^*/\mu^{(e)}\simeq10$, and the response of earth model P is again predominantly determined by $\mu^{(e)}$. Hence, the values of $T^{(e)}$, $T^{(v)}$ and β^{-1} are similar to those for earth model R. At the same time, since the values of $\mu^{(e)}$ and κ^* are larger by a factor of 10 than the values used in Fig. 4 (bottom), the elastic amplitudes remain smaller. The effect of reducing κ^* to 1×10^{11} Pa is shown in Fig. 5 (bottom). Now, $\kappa^*/\mu^{(e)}<1$, which means that the response of earth model P is strongly influenced by its compressibility. The effects caused by compressibility shown in Fig. 4 (top) are thus even more pronounced and, in particular, the overshoot of $T^{(e)}$ for small n is prominent. However, values of κ smaller than those of μ are not encountered in the earth and the result is thus mainly of theoretical interest.

4.3.3 Earth model C

As for earth models R and P, $T^{(e)}$ can be calculated analytically for earth model C and $T^{(v)}$ is given as $1-T^{(e)}$. However, since the response of earth model C is not characterized by exponential decay, the relaxation time is not defined and the behaviour in time must be discussed using $T^{(ve)}$.

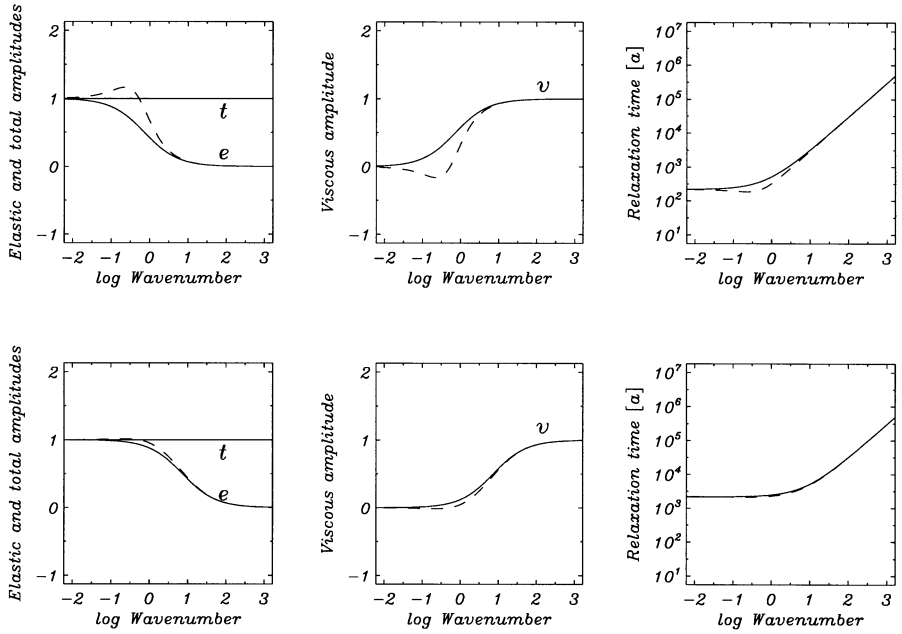

Figure 4. Elastic amplitude, $T^{(e)}$, viscous amplitude, $T^{(v)}$, total amplitude, $T^{(e)}+T^{(v)}$, and relaxation time, β^{-1}, as functions of the normalized Hankel wavenumber, n, for earth model R (solid) and earth model P (dashed). Results apply to $\mu^{(e)}=1.45\times10^{11}$ Pa (top) and $\mu^{(e)}=1.45\times10^{10}$ Pa (bottom); the other parameter values are given in Table 1.

Fig. 6 shows effects due to variations of λ; the other parameters have their standard values (Table 1). In Fig. 6 (top), $\lambda=8.81\times10^{-4}$ kg m^{-4} applies. Then, earth models R and C show similar values of $T^{(e)}$ down to $n\simeq10$. If n becomes still smaller, the compositional density gradient leads to a pronounced reduction of $T^{(e)}$. Its maximum is near $n=1$ and it approaches 0 for $n\to0$. For $n<10$, the relaxation for earth model C is strongly retarded in comparison to earth model R. In Fig. 6 (bottom), λ is reduced to 8.81×10^{-6} kg m^{-4}. Now, significant discrepancies between the responses of earth models R and C are limited to $n<1$, which is beond the range of applicability of the half-space approximation.

Physically, the slower relaxation associated with a compositional density gradient is due to a retarding force. Thus, if a surface load deforms earth model C, particles below the load are displaced to greater depths than particles further away from the load. This gives rise to a lateral density gradient away from the load centre and thus to a buoyancy force, which counteracts the vertical displacement.

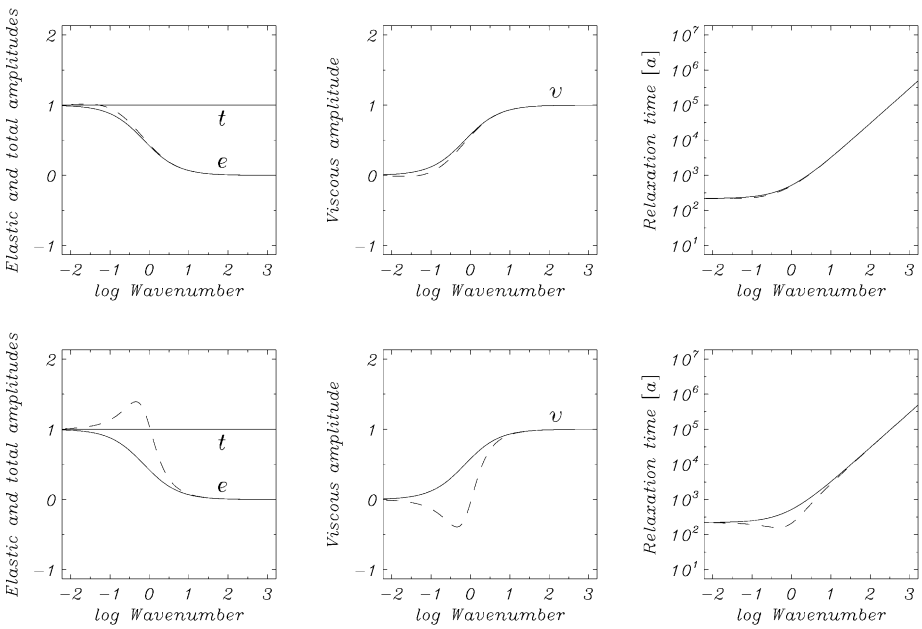

Figure 5. Elastic amplitude, $T^{(e)}$, viscous amplitude, $T^{(v)}$, total amplitude, $T^{(e)}+T^{(v)}$, and relaxation time, β^{-1}, as functions of the normalized Hankel wavenumber, n, for earth model R (solid) and earth model P (dashed). Results apply to $\kappa^*=2.00\times10^{12}$ Pa (top) and $\kappa^*=1.00\times10^{11}$ Pa (bottom); the other parameter values are given in Table 1.

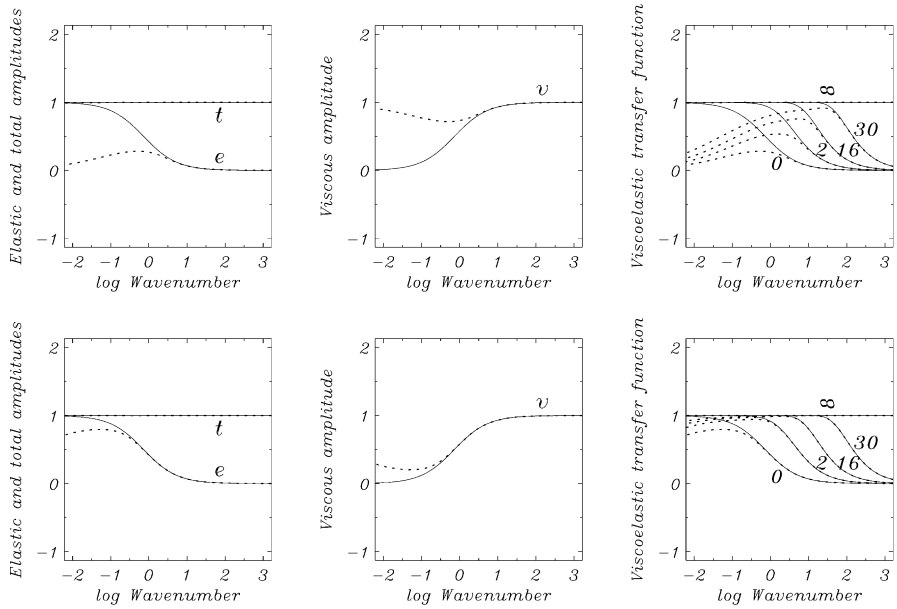

Figure 6. Elastic amplitude, $T^{(e)}$, viscous amplitude, $T^{(v)}$, total amplitude, $T^{(e)}+T^{(v)}$, and viscoelastic transfer function, $T^{(ve)}$, as functions of the normalized Hankel wavenumber, n, for earth model R (solid) and earth model C (dotted). Numbers denote times (in units of ka) after onset of loading. Results apply to $\lambda=8.81\times10^{-4}$ kg m^{-4} (top) and $\lambda=8.81\times10^{-6}$ kg m^{-4} (bottom); the other parameter values are given in Table 1.

4.4 Computational results: (r, z, t) domain

Next, the vertical surface displacement for earth models R, P and C in the (r, z, t) domain is calculated and discussed. This requires that the load cross-section be specified and the inverse Hankel transformation be implemented.

4.4.1 Load cross-section

In order to obtain crude approximations of the major Pleistocene ice sheets in Fennoscandia and Canada, we choose circular disc loads with elliptical load cross-sections. With h_L the maximum load thickness, r_L the load radius and ρ_L the load density, we thus have

$$\sigma'(r)=\rho_L h_L\begin{cases}\sqrt{1-\left(\dfrac{r}{r_L}\right)^2}, & 0\le r<r_L,\\ 0, & r_L<r<\infty.\end{cases}\tag{87}$$

Its zeroth-order Hankel transform is (e.g. Farrell 1982)

$$\Sigma'(k)=\rho_L h_L\,\frac{r_L}{k}\,j_1(kR),\tag{88}$$

where $j_1(x)=\sin x/x^2-\cos x/x$ is the spherical Bessel function of the first kind (e.g. Abramowitz & Stegun 1965, pp. 437–438). The lth-order inverse Hankel transform given by

$$f(r)=\int_0^\infty F^{[l]}(k)J_l(kr)\,k\,dk\tag{89}$$

is evaluated numerically for $F(k)=[W(k)]_+=T^{(ve)}(k)\Sigma'(k)/\rho^*$.

4.4.2 Discussion

Fig. 7 shows the vertical surface displacement, $[w]_+$, as a function of radial distance, r, caused by loads with elliptical cross-sections. The parameters are $\rho_L=1000$ kg m^{-3} and $h_L=2$ km, $r_L=800$ km (Fennoscandian ice load, top) or $h_L=3$ km, $r_L=1600$ km (Canadian ice load, bottom); as above, a Heaviside loading history is assumed. The parameters of the three earth models considered are given in Table 1.

Near the load axis, $[w]_+$ is always *larger* for earth model P than for earth model R. The maximum differences amount to $\sim$10 m (Fennoscandia) or $\sim$35 m (Canada) and are reached before 5 ka after the onset of loading. After about 10 ka, the differences have essentially vanished. In contrast to this is the relaxation of earth model C, for which $[w]_+$ is *smaller* than for earth model R. Near the load axis, the maximum differences reach $\sim$50 m (Fennoscandia) or $\sim$150 m (Canada) shortly after 5 ka. At later times, the differences diminish and vanish in the final state of hydrostatic equilibrium.

Earth model P relaxes faster than earth model R also in the region peripheral to the load. However, the differences in $[w]_+$ are smaller than in the central region and usually remain below 5 m (Fennoscandia) or 15 m (Canada). In contrast to this are the responses of earth models C and R, which continue to show prominent differences in the peripheral region. As a consequence of its longer relaxation time, $[w]_+$ for earth model C may be reduced by as much as 15 m (Fennoscandia) or 50 m (Canada).

The result that $[w]_+$ is identical for the three earth models in the final state of hydrostatic equilibrium can be understood from the fact that, for a given load, the surface displacement in this limit is solely controlled by the product ρ^*g. Since $\rho^*=3380$ kg m^{-3} for each of the earth models used, the differences must therefore vanish in this limit.

5 CONCLUDING REMARKS

The main results of this study are the following.

(1) We have developed the theory governing viscoelastic perturbations of a half-space with an initial density gradient due to both *compressional* and *compositional* stratification.

(2) For the special case of a purely compressional or a purely compositional density gradient, *closed-form* solutions

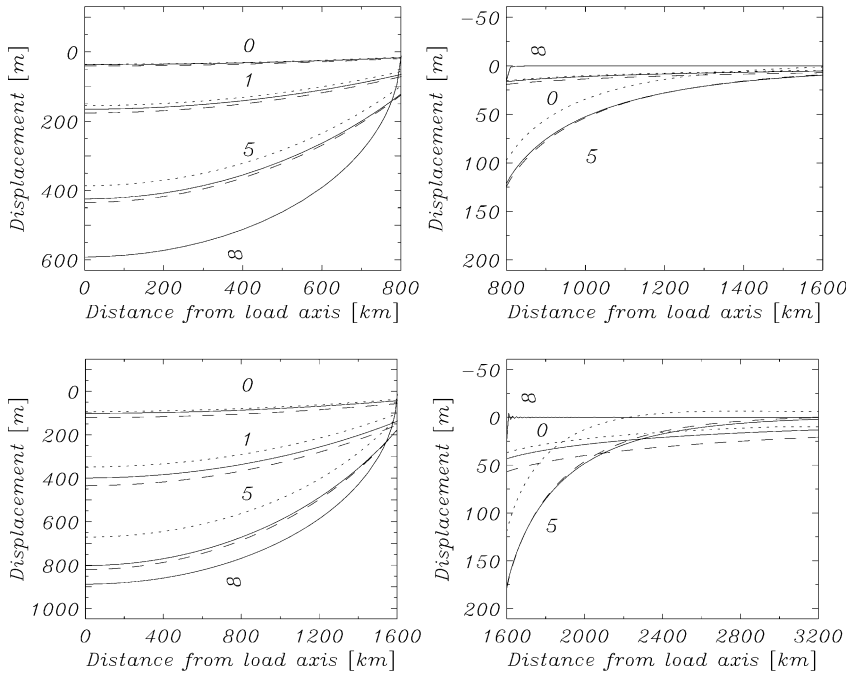

Figure 7. Vertical surface displacement, $[w]_+$, as a function of distance, r, from the load axis for earth model R (solid), earth model P (dashed) and earth model C (dotted). Numbers denote times (in units of ka) after onset of loading. Results apply to elliptical load cross-section with $h_L = 2$ km, $r_L = 800$ km (top), $h_L = 3$ km, $r_L = 1600$ km (bottom) and $\rho_L = 1000$ kg m^{-3}.

for the incremental fields have been obtained in the (k, z, s) domain. For compressional stratification, the inverse Laplace transform can be implemented *analytically* and leads to a relaxation characterized by an exponentially decaying normal mode. On the other hand, for compositional stratification the transcendental character of the transfer function to be inverted requires the use of *numerical* methods.

(3) Computational results in the (k, z, t) domain for the surface of the half-space show that effects due to the density stratification on the vertical displacement are limited to *low wavenumber* deformations and only become prominent for normalized wavenumbers smaller than ~ 10. Compared to the special case of a half-space with spatially homogeneous density, vertical displacements are enhanced for compressional density stratification and reduced for compositional stratification.

(4) Computational results in the (r, z, t) domain and for disc loads with dimensions typical of the *Pleistocene ice sheets* in Fennoscandia and Canada show that the vertical surface displacement may deviate from that for spatially homogeneous density by ~ 10 m and ~ 35 m, respectively (compressional stratification) and by ~ 50 m and ~ 150 m, respectively (compositional stratification). Whereas compressibility leads to an *enhancement* of the displacement, the internal buoyancy associated with a compositional density increase results in a *reduction* of the displacement. These deviations represent *upper limits*, since the effects partially compensate each other if both compressional and compositional density stratifications are present.

(5) Since the influence of the density stratification on the displacement is limited to low wavenumber deformations, the neglect of *sphericity* and *self-gravitation* effected in this investigation should be justified more carefully in the future. The next step would therefore be to extend our study to gravitationally self-consistent spherical earth models. At the same time, this extension may illuminate the physics of the overshoots observed for the elastic response of compressionally stratified half-spaces.

ACKNOWLEDGMENTS

Constructive comments by L. Ballani, G. Li, E. Ivins, P. Johnston, C. Matyska, M. Nakada and P. Wu are gratefully acknowledged.

REFERENCES

Abramowitz, M. & Stegun, I.A., 1965. *Handbook of Mathematical Functions,* Dover, New York.

Adams, L.H. & Williamson, E.D., 1925. The composition of the earth's interior, in *Annual Report of the Smithsonian Institute 1922/23,* pp. 241–260, Smithsonian Institution, Washington.

Amelung, F. & Wolf, D., 1994. Viscoelastic perturbations of the earth: significance of the incremental gravitational force in models of glacial isostasy, *Geophys. J. Int.,* **117,** 864–879.

Birch, F., 1952. Elasticity and constitution of the earth's interior, *J. Geophys. Res.,* **57,** 227–286.

Birch, F., 1964. Density and composition of mantle and core, *J. Geophys. Res.,* **69,** 4377–4388.

Bullen, K.E., 1975. *The Earth's Density,* Chapman & Hall, London.

Cathles, L.M., 1975 *The Viscosity of the Earth's Mantle,* Princeton University Press, Princeton.

Dziewonski, A.M. & Anderson, D.L., 1981. Preliminary reference earth model, *Phys. Earth planet. Inter.,* **25,** 279–356.

Fang, M. & Hager, B.H., 1994. A singularity free approach to post glacial rebound calculations, *Geophys. Res. Lett.,* **21,** 2131–2134.

Fang, M. & Hager, B.H., 1995. The singularity mystery associated with a radially continuous Maxwell viscoelastic structure, *Geophys. J. Int.,* **123,** 849–865.

Farrell, W.E., 1972. Deformation of the earth by surface loads, *Rev. Geophys. Space Phys.,* **10,** 761–797.

Gantmacher, F.R., 1959. *The Theory of Matrices,* Vol. 1, Chelsea, New York.

Han, D. & Wahr, J., 1995. The viscoelastic relaxation of a realistically stratified earth, and a further analysis of postglacial rebound, *Geophys. J. Int.,* **120,** 287–311.

Hanyk, L., Moser, J., Yuen, D.A. & Matyska, C., 1995. Time-domain approach for the transient responses in stratified viscoelastic earth models, *Geophys. Res. Lett.,* **22,** 1285–1288.

Hanyk, L., Matyska, C. & Yuen, D.A., 1999. Secular gravitational instability of a compressible viscoelastic sphere, *Geophys. Res. Lett.,* **26,** 557–560.

LePage, W.R., 1980. *Complex Variables and the Laplace Transform for Engineers,* Dover, New York.

Li, G. & Yuen, D.A., 1987. Viscous relaxation of a compressible spherical shell, *Geophys. Res. Lett.,* **14,** 1227–1230.

Mitrovica, J.X. & Peltier, W.R., 1992. A comparison of methods for the inversion of viscoelastic relaxation spectra, *Geophys. J. Int.,* **108,** 410–414.

Panasyuk, S.V., Hager, B.H. & Forte, A.M., 1996. Understanding the effects of mantle compressibility on geoid kernels, *Geophys. J. Int.,* **124,** 121–133.

Parsons, B.E., 1972. Changes in the earth's shape, *PhD thesis,* Cambridge University, Cambridge.

Peltier, W.R., 1974. The impulse response of a Maxwell earth, *Rev. Geophys. Space Phys.,* **12,** 649–669.

Sneddon, I.N., 1951. *Fourier Transforms,* McGraw-Hill, New York.

Thoraval, C., Machetel, P. & Cazenave, A., 1994. Influence of mantle compressibility and ocean warping on dynamical models of the geoid, *Geophys. J. Int.,* **117,** 566–573.

Vermeersen, L.L.A. & Sabadini, R., 1998. Effects of compressibility and stratification on viscoelastic relaxation: the analytical perspective, in *Dynamics of the Ice Age Earth: A Modern Perspective,* pp. 123–134, ed. Wu, P., Trans Tech Publications, Uetikon.

Vermeersen, L.L.A., Sabadini, R. & Spada, G., 1996a. Compressional rotational deformation, *Geophys. J. Int.,* **126,** 735–761.

Vermeersen, L.L.A., Sabadini, R. & Spada, G., 1996b. Analytical visco-elastic relaxation models, *Geophys. Res. Lett.,* **23,** 697–700.

Wieczerkowski, K., 1999. Gravito-Viskoelastodynamik für verallgemeinerte Rheologien mit Anwendungen auf den Jupitermond Io und die Erde, *PhD thesis,* University of Münster, Germany.

Williamson, E.D. & Adams, L.H., 1923. Density distribution in the earth, *J. Washington Acad. Sci.,* **13,** 413–428.

Wolf, D., 1985a. The normal modes of a uniform, compressible Maxwell half-space, *J. Geophys.,* **56,** 100–105.

Wolf, D., 1985b. Thick-plate flexure re-examined, *Geophys. J. R. astr. Soc.,* **80,** 265–273

Wolf, D., 1985c. On Boussinesq's problem for Maxwell continua subject to an external gravity field, *Geophys. J. R. astr. Soc.,* **80,** 275–279.

Wolf, D., 1991a. Viscoelastodynamics of a stratified, compressible planet: incremental field equations and short- and long-time asymptotes, *Geophys. J. Int.,* **104,** 401–417.

Wolf, D., 1991b. Boussinesq's problem of viscoelasticity, *Terra Nova,* **3,** 401–407.

Wolf, D., 1994. Lamé's problem of gravitational viscoelasticity: the isochemical, incompressible planet, *Geophys. J. Int.,* **116,** 321–348.

Wolf, D., 1997. Gravitational viscoelastodynamics for a hydrostatic planet, Veröff. Deut. Geod. Komm., **C452**.

Wu, J. & Yuen, D.A., 1991. Postglacial relaxation of a viscously stratified compressible mantle, *Geophys. J. Int.,* **104,** 331–349.

Wu, P. & Peltier, W.R., 1982. Viscous gravitational relaxation, *Geophys. J. R. astr. Soc.,* **70,** 435–485.

APPENDIX A: LIST OF IMPORTANT SYMBOLS

A1 Latin symbols

a	earth radius
c	composition
d_t	material time-derivative operator
e	2.71828 ...
f	scalar function or field
f^*	surface value of f or $f^{(0)}$
$F_{ij}^{[l]}$	lth-order Hankel transform of f_{ij}
f_{ij}	Cartesian tensor field
$f_{ij,k}$	material gradient of f_{ij}
$\tilde{f}_{ij}$	Laplace transform of f_{ij}
$f_{ij}^{(0)}$	initial value of f_{ij}
$f_{ij}^{(\Delta)}$	local incremental value of $f_{ij}^{(0)}$
$f_{ij}^{(\delta)}$	material incremental value of $f_{ij}^{(0)}$
g_i	gravity
H	Heaviside step function
h_{L}	maximum load thickness
i	imaginary unit
k	Hankel wavenumber
m	eigenvalue
n	normalized Hankel wavenumber
n_i	unit normal in direction of g_i
p	mechanical pressure
r	radial distance
r_i	current particle position
r_{L}	load radius
s	Laplace frequency
$T^{(\mathrm{e})}$	elastic amplitude
$T^{(\mathrm{v})}$	viscous amplitude
$T^{(\mathrm{ve})}$	viscoelastic transfer function
t	current time
t'	excitation time
t_{ij}	Cauchy stress
u	radial displacement
u_i	displacement
w	downward displacement
X_i	initial particle position
z	depth

A2 Greek symbols

α	inverse Maxwell time
β	inverse relaxation time
γ_i	inverse compressional scale length
δ	compositional coefficient
δ_{ij}	Kronecker symbol
ϵ	compressional coefficient
η	viscosity
κ	isentropic bulk modulus
λ_i	compositional density gradient
μ	shear-relaxation function
$\mu^{(\mathrm{e})}$	elastic shear modulus
ξ	state function
ρ	volume mass density
ρ_{L}	load density
σ	incremental interface mass density
τ_i	non-isentropic temperature gradient
ϕ	azimuth
χ	thermal expansivity
ω	rotation

A3 Calligraphic symbols

$\mathscr{X}^2$	2-D domain of X_i
$\mathscr{X}^3$	3-D domain of X_i